A General Contact Model for Dynamically-Decoupled Force/Motion Control

Roy Featherstone*
Department of Engineering Science
Oxford University
Parks Road, Oxford OX1 3PJ, England
roy@robots.oxford.ac.uk
Stef Sonck
Aerospace Robotics Laboratory
Department of Aeronautics and Astronautics
Stanford University
Stanford, CA 94305, USA
ssonck@sun-valley.Stanford.EDU
Oussama Khatib
Robotics Laboratory
Department of Computer Science
Stanford University
Stanford, CA 94305, USA
khatib@cs.Stanford.EDU

Abstract: This paper presents a general first-order kinematic model of frictionless rigid-body contact for use in hybrid force/motion control. It is formulated in an invariant manner by treating motion and force vectors as members of two separate but dual vector spaces. The more general kinematics allows us to model tasks that cannot be described using the Raibert-Craig model; a single Cartesian frame in which directions are either force- or motion-controlled is not sufficient. The model can be integrated with the object and manipulator dynamics in order to model both the kinematics and dynamics of contact. These equations of motion can be used to design force and motion controllers in the appropriate subspaces. To guarantee decoupling between the controllers, it is possible to apply projection matrices to the controller outputs that depend solely on the kinematic model of contact, not a dynamic one. Experimental results show a manipulation that involves controlling the force in two separate face-vertex contacts while performing motion. These multi-contact compliant motions often occur as part of an assembly and cannot be described using the Raibert-Craig model.

*Supported by EPSRC Advanced Research Fellowship number B92/AF/1466.

1. Introduction

The modern concept of hybrid control, as described in the work of Raibert and Craig [15], has attracted a great deal of interest over the years. In addition to the various improvements, extensions and practical implementations that have been proposed, two theoretical errors in the original formulation have received attention: the non-invariant formulation of the original contact model [5, 12] and the phenomenon of kinematic instability caused by an incorrect filtering of error signals into force and motion components [1, 8, 18].

Another problem with the Raibert-Craig model, which appears to have been neglected, is that it lacks sufficient generality to describe an arbitrary state of contact between two rigid bodies. Other published models vary on this point: some suffer the same problem (*e.g.* [4, 6, 10]) while others are completely general (*e.g.* [2, 3, 9, 16, 17]).

This paper is organized as follows. First, we show that the Raibert-Craig model is not general and give two examples of contacts that it can not handle. Then, after a brief review of dual vector systems, we describe the new model. This model can describe any (non-singular) state of frictionless contact between two rigid bodies. Force and motion filtering is accomplished by projection matrices that are invariant with respect to choice of units and coordinate systems; and it can be shown that these matrices are kinematically stable, although this subject is not discussed in this paper.

The next section combines the kinematic model with the dynamics of the manipulator and environment. It presents an analysis of the equations of motion of a manipulator in contact using the projection matrices derived earlier. It is possible to guarantee that a force/motion controller exhibits dynamically decoupled behavior (*i.e.*, the actual contact force and acceleration depend only on the outputs of the respective force and motion controller) using projection matrices that depend solely on the kinematic model of contact.

To validate the theory, we present experimental results showing a robot performing a compliant motion task that can not be described by the Raibert-Craig model. The task involves controlling the contact force between the manipulated object and the environment in two face-vertex contacts, while executing a motion.

2. Generality of Contact Models for Force/Motion Control

A state of contact between a robot's end effector and its environment defines a constraint surface in the robot's operational space such that all points on the surface satisfy the contact constraints. At any given instant, this surface defines two vector spaces: a space of tangent vectors containing all permissible motions (velocities, infinitesimal displacements, or accelerations after compensation for velocity-product effects), and a space of normal vectors containing all permissible contact forces. A mathematical model of contact must include a means of describing these two spaces.

The contact model used by Raibert and Craig was based on the theoretical work of Mason [13], and consists of a Cartesian coordinate frame, called the constraint frame, and a compliance selection matrix. This model is character-

ized by six geometric parameters, giving the position and orientation of the constraint frame, and six binary parameters to select motion or force control in each direction. Unfortunately, any contact model that uses only six geometric parameters is lacking in generality.

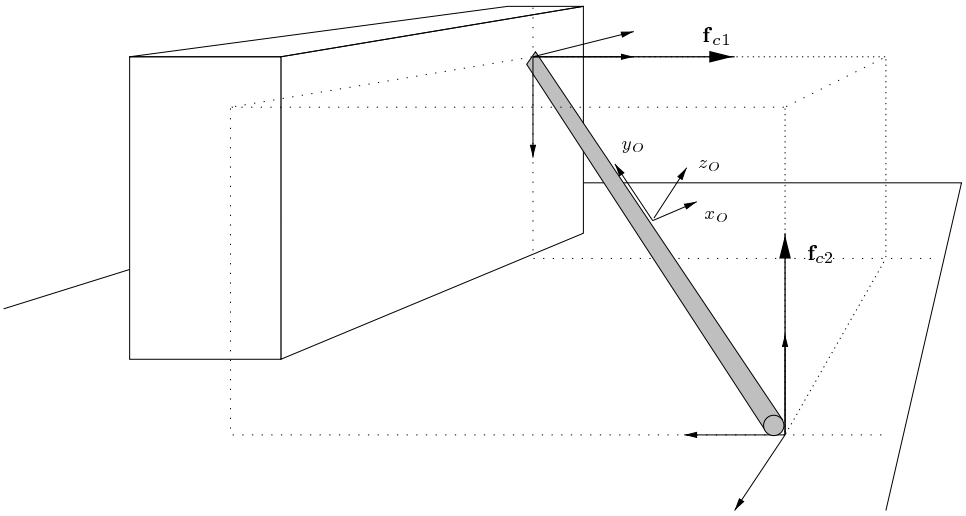

Figure 1. A general two-point contact with skew, non-intersecting contact normals.

Figures 1 and 2 show examples of contact states that can not be described by the Raibert-Craig model. For example, in figure 1 it is not possible to find a location for the constraint frame such that the space spanned by the two contact normals along forces $\mathbf{f}_{c1}$ and $\mathbf{f}_{c2}$ equals a space spanned by two constraint-frame directions.

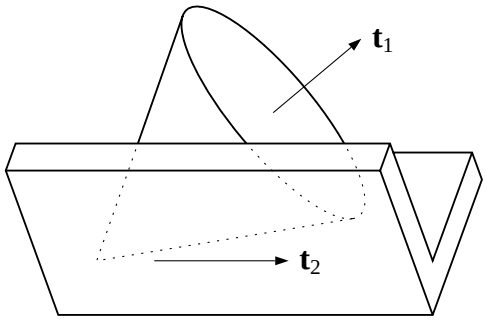

Figure 2. A cone with two motion freedoms: rotation about its axis ($\mathbf{t}_1$) and translation along the groove's axis ($\mathbf{t}_2$). The two axes are neither parallel nor perpendicular.

3. Dual Vector Spaces

In this section, we briefly review the mathematics of dual vector spaces. The basic idea is that we have two separate vector spaces, one containing force-type vectors, and the other containing motion-type vectors. We shall call them F^6 and M^6. The scalar product defined between them is called the reciprocal product; it is the work done by a force-type vector acting on a motion-type vector.

A Cartesian coordinate frame defines two separate bases: $\{f_1 \dots f_6\}$ for F^6 and $\{m_1 \dots m_6\}$ for M^6. The abstract vectors $f \in \mathsf{F}^6$ and $v \in \mathsf{M}^6$ are represented by the column matrices $\mathbf{f}$ and $\mathbf{v}$ in these bases. The basis vectors must satisfy the reciprocity condition

$$f_i \cdot m_j = \begin{cases} 1\,W & \text{if } i = j \\ 0 & \text{otherwise} \end{cases},$$

where W is the appropriate unit of work. This condition enforces consistency of units and ensures that the scalar product $f \cdot v$ can be expressed as $\mathbf{f}^T\mathbf{v}$. By convention, the two bases comprise three unit forces, three unit couples, three unit linear motions and three unit angular motions.

If $\mathbf{f}_P$, $\mathbf{f}_Q$, $\mathbf{v}_P$ and $\mathbf{v}_Q$ are representations of f and v in Cartesian coordinate frames P and Q, and $\mathbf{X}_f$ and $\mathbf{X}_m$ are coordinate transformation matrices from P to Q coordinates for force-type and motion-type vectors, respectively, then

$$\mathbf{v}_Q = \mathbf{X}_m\,\mathbf{v}_P, \qquad \mathbf{v}_P = \mathbf{X}_m^{-1}\,\mathbf{v}_Q, \tag{1}$$

$$\mathbf{f}_Q = \mathbf{X}_f\,\mathbf{f}_P, \qquad \mathbf{f}_P = \mathbf{X}_f^{-1}\,\mathbf{f}_Q. \tag{2}$$

The transformational properties of the two spaces are constrained by the need to preserve invariance of $\mathbf{f}^T\mathbf{v}$:

$$\mathbf{X}_f = (\mathbf{X}_m^{-1})^T. \tag{3}$$

Given the two vector spaces, we can define four types of linear mapping between them. Physical examples are: inertia, inverse inertia, force projection and motion projection, respectively. To preserve invariance, these mappings must transform as follows.

$$\mathsf{M}^6 \mapsto \mathsf{F}^6 \;:\; \mathbf{A}_Q = \mathbf{X}_f\,\mathbf{A}_P\,\mathbf{X}_m^{-1}, \tag{4}$$

$$\mathsf{F}^6 \mapsto \mathsf{M}^6 \;:\; \mathbf{B}_Q = \mathbf{X}_m\,\mathbf{B}_P\,\mathbf{X}_f^{-1}, \tag{5}$$

$$\mathsf{F}^6 \mapsto \mathsf{F}^6 \;:\; \mathbf{C}_Q = \mathbf{X}_f\,\mathbf{C}_P\,\mathbf{X}_f^{-1}, \tag{6}$$

$$\mathsf{M}^6 \mapsto \mathsf{M}^6 \;:\; \mathbf{D}_Q = \mathbf{X}_m\,\mathbf{D}_P\,\mathbf{X}_m^{-1}. \tag{7}$$

4. A General First-order Model of Contact

A general state of contact between two rigid bodies defines a constraint surface in their relative configuration space. At any given instant, this surface defines two vector spaces: an r-dimensional space of contact normal vectors $N \subseteq \mathsf{F}^6$ and a $(6-r)$-dimensional space of tangent vectors $T \subseteq \mathsf{M}^6$, where r is the

degree of motion constraint. These spaces can be modeled by means of a $6 \times r$ matrix $\mathbf{N}$ and a $6 \times (6-r)$ matrix $\mathbf{T}$ such that

$$N = \text{range}(\mathbf{N}), \quad T = \text{range}(\mathbf{T}).$$

The columns of $\mathbf{N}$ are any r linearly independent force vectors in N, and the columns of $\mathbf{T}$ are any $6-r$ linearly independent motion vectors in T. There is no need for any of these vectors to be normalized or orthogonal in any sense.

One of the basic properties of a contact constraint is that a constraint force does no work against an infinitesimal displacement that is consistent with the constraint. In other words, the scalar product of any member of N with any member of T is zero. This property can be expressed as $N \perp T$ or, in terms of matrices,

$$\mathbf{N}^T \mathbf{T} = \mathbf{0}.$$

In many situations, a suitable value for $\mathbf{N}$, $\mathbf{T}$ or both can be obtained by inspection. For the contact shown in Figure 1, a suitable value for $\mathbf{N}$ is $\mathbf{N} = [\mathbf{f}_{c1}\ \mathbf{f}_{c2}]$; and for the contact shown in Figure 2, a suitable value for $\mathbf{T}$ is $\mathbf{T} = [\mathbf{t}_1\ \mathbf{t}_2]$.

5. The Projection Matrices

Let us introduce two more spaces, N' and T', and their matrix representations $\mathbf{N}'$ and $\mathbf{T}'$, satisfying

$$N \oplus N' = \mathsf{F}^6, \quad T \oplus T' = \mathsf{M}^6,$$

where $\oplus$ means direct sum. N' can be any $(6-r)$-dimensional force subspace with no non-zero element in common with N, and T' can be any r-dimensional motion subspace with no non-zero element in common with T. It is important to recognize that N' and T' are not defined by the contact.

Each possible value of N' defines a unique decomposition of a general force vector into components in N and N'. Similarly, each possible value of T' defines a unique decomposition of a general motion vector into components in T and T'. Thus, given $f \in \mathsf{F}^6$ and $v \in \mathsf{M}^6$, we have

$$\mathbf{f} = \mathbf{f}_1 + \mathbf{f}_2 = \mathbf{N}\,\boldsymbol{\alpha}_1 + \mathbf{N}'\,\boldsymbol{\alpha}_2, \tag{8}$$

$$\mathbf{v} = \mathbf{v}_1 + \mathbf{v}_2 = \mathbf{T}\,\boldsymbol{\beta}_1 + \mathbf{T}'\,\boldsymbol{\beta}_2, \tag{9}$$

where $\boldsymbol{\alpha}_1$, $\boldsymbol{\alpha}_2$, $\boldsymbol{\beta}_1$ and $\boldsymbol{\beta}_2$ are all uniquely determined.

We are now in a position to define the projection matrices, $\boldsymbol{\Omega}_f$ and $\bar{\boldsymbol{\Omega}}_f$, which split a force vector $\mathbf{f}$ into its components $\mathbf{f}_1 = \boldsymbol{\Omega}_f \mathbf{f} \in N$ and $\mathbf{f}_2 = \bar{\boldsymbol{\Omega}}_f \mathbf{f} \in N'$, and the motion projection matrices $\boldsymbol{\Omega}_m$ and $\bar{\boldsymbol{\Omega}}_m$ that act similarly on $\mathbf{v}$. These projections are not uniquely defined by N and T, but also depend on N' and T'. After a little algebraic manipulation, the results are

$$\bar{\boldsymbol{\Omega}}_f = \mathbf{N}'\,(\mathbf{T}^T\,\mathbf{N}')^{-1}\,\mathbf{T}^T = \mathbf{1} - \boldsymbol{\Omega}_f, \tag{10}$$

$$\bar{\boldsymbol{\Omega}}_m = \mathbf{T}'\,(\mathbf{N}^T\,\mathbf{T}')^{-1}\,\mathbf{N}^T = \mathbf{1} - \boldsymbol{\Omega}_m. \tag{11}$$

$\boldsymbol{\Omega}_f$ and $\bar{\boldsymbol{\Omega}}_f$ are both force-to-force mappings, and therefore transform according to Eq. 6. Similarly, $\boldsymbol{\Omega}_m$ and $\bar{\boldsymbol{\Omega}}_m$ transform according to Eq. 7.

Equations 10 and 11 express every possible invariant projection matrix that is consistent with the given contact constraint. Without loss of generality, it is possible to represent N' and T' in the form

$$N' = \mathbf{A}\, T = \text{range}(\mathbf{A}\, \mathbf{T}), \quad T' = \mathbf{B}\, N = \text{range}(\mathbf{B}\, \mathbf{N}),$$

where $\mathbf{A}$ and $\mathbf{B}$ are positive-definite 6×6 matrices representing linear mappings from M^6 to F^6 and F^6 to M^6 respectively. To preserve invariance, $\mathbf{A}$ must transform like inertia (Eq. 4) and $\mathbf{B}$ like inverse inertia (Eq. 5). Using this representation, all possible projection matrices for a given contact constraint can be expressed as

$$\begin{aligned}
\boldsymbol{\Omega}_f(\mathbf{A}) &= \mathbf{N}\,(\mathbf{N}^T\,\mathbf{A}^{-1}\,\mathbf{N})^{-1}\,\mathbf{N}^T\,\mathbf{A}^{-1} &&= \mathbf{N}\,\mathbf{N}^{\#}_{\mathbf{A}^{-1}}\,, && (12)\\
\bar{\boldsymbol{\Omega}}_f(\mathbf{A}) &= \mathbf{A}\,\mathbf{T}\,(\mathbf{T}^T\,\mathbf{A}\,\mathbf{T})^{-1}\,\mathbf{T}^T &&= \mathbf{1} - \boldsymbol{\Omega}_f(\mathbf{A})\,, && (13)\\
\boldsymbol{\Omega}_m(\mathbf{B}) &= \mathbf{T}\,(\mathbf{T}^T\,\mathbf{B}^{-1}\,\mathbf{T})^{-1}\,\mathbf{T}^T\,\mathbf{B}^{-1} &&= \mathbf{T}\,\mathbf{T}^{\#}_{\mathbf{B}^{-1}}\,, && (14)\\
\bar{\boldsymbol{\Omega}}_m(\mathbf{B}) &= \mathbf{B}\,\mathbf{N}\,(\mathbf{N}^T\,\mathbf{B}\,\mathbf{N})^{-1}\,\mathbf{N}^T &&= \mathbf{1} - \boldsymbol{\Omega}_m(\mathbf{B})\,. && (15)
\end{aligned}$$

Some useful relationships are independent of the choice of $\mathbf{A}$ or $\mathbf{B}$:

$$\begin{aligned}
\boldsymbol{\Omega}_f(\mathbf{A}_1)\,\boldsymbol{\Omega}_f(\mathbf{A}_2) &= \boldsymbol{\Omega}_f(\mathbf{A}_2), && (16)\\
\bar{\boldsymbol{\Omega}}_f(\mathbf{A}_1)\,\boldsymbol{\Omega}_f(\mathbf{A}_2) &= 0, && (17)\\
\boldsymbol{\Omega}_m(\mathbf{B}_1)\,\boldsymbol{\Omega}_m(\mathbf{B}_2) &= \boldsymbol{\Omega}_m(\mathbf{B}_2), && (18)\\
\bar{\boldsymbol{\Omega}}_m(\mathbf{B}_1)\,\boldsymbol{\Omega}_m(\mathbf{B}_2) &= 0. && (19)
\end{aligned}$$

6. Combining the Contact Model with Dynamics

The basic operational-space equation of motion for the object and the manipulator(s) (i.e. the augmented object model) [11] is

$$\boldsymbol{\Lambda}_0(\mathbf{x})\,\dot{\boldsymbol{\vartheta}} + \boldsymbol{\mu}_0(\mathbf{x}, \boldsymbol{\vartheta}) + \mathbf{p}_0(\mathbf{x}) + \mathbf{f}_c = \mathbf{f} \tag{20}$$

where $\mathbf{x}$ is a vector of operational-space coordinates, $\boldsymbol{\vartheta}, \dot{\boldsymbol{\vartheta}} \in \mathsf{M}^6$ are end-effector velocity and acceleration vectors, $\boldsymbol{\Lambda}_0$ is the operational-space inertia matrix, $\boldsymbol{\mu}_0, \mathbf{p}_0 \in \mathsf{F}^6$ are vectors of velocity-product and gravitational terms, $\mathbf{f}_c \in \mathsf{F}^6$ is the contact force applied by the robot to the environment, and $\mathbf{f} \in \mathsf{F}^6$ is the force command to the robot. We model the environment by the equation of motion

$$\mathbf{a}_e = \boldsymbol{\Phi}_e\,\mathbf{f}_c + \mathbf{b}_e. \tag{21}$$

$\mathbf{a}_e$ is the environment's acceleration, $\boldsymbol{\Phi}_e$ is its inverse inertia (a positive semidefinite matrix), and $\mathbf{b}_e$ is its bias acceleration (the acceleration it would have in the absence of a contact force) [7]. Eq. 21 models any environment that accepts an arbitrary applied force, and is functionally equivalent to the model used in [3]. A fixed, stationary environment can be modeled with $\boldsymbol{\Phi}_e = \mathbf{0}$, $\mathbf{b}_e = \mathbf{0}$.

The contact imposes constraints on the relative acceleration between the end effector and environment, and on the contact force. These constraints are

$$\dot{\boldsymbol{\vartheta}}' = \mathbf{T}\,\dot{\boldsymbol{\beta}}, \tag{22}$$

$$\mathbf{f}_c = \mathbf{N}\,\boldsymbol{\alpha}, \tag{23}$$

where $\dot{\boldsymbol{\beta}}$ and $\boldsymbol{\alpha}$ are unknown acceleration and force vectors, and $\dot{\boldsymbol{\vartheta}}'$ is the relative acceleration with the velocity-product terms removed:

$$\dot{\boldsymbol{\vartheta}}' = \dot{\boldsymbol{\vartheta}} - \mathbf{a}_e - \dot{\mathbf{T}}\,\boldsymbol{\beta}.$$

Combining Eqs. 20–22 and rearranging gives

$$\dot{\boldsymbol{\beta}} = (\mathbf{T}^T \boldsymbol{\Lambda}_{rel}\,\mathbf{T})^{-1}\,\mathbf{T}^T\,\boldsymbol{\Lambda}_{rel}\,\boldsymbol{\Lambda}_0^{-1}\,\mathbf{f}', \tag{24}$$

$$\boldsymbol{\alpha} = (\mathbf{N}^T \boldsymbol{\Lambda}_{rel}^{-1}\mathbf{N})^{-1}\,\mathbf{N}^T\boldsymbol{\Lambda}_0^{-1}\,\mathbf{f}', \tag{25}$$

where

$$\mathbf{f}' \triangleq \mathbf{f} - \boldsymbol{\mu}_0 - \mathbf{p}_0 - \boldsymbol{\Lambda}_0\,(\dot{\mathbf{T}}\,\boldsymbol{\beta} + \mathbf{b}_e),$$

and

$$\boldsymbol{\Lambda}_{rel} \triangleq (\boldsymbol{\Lambda}_0^{-1} + \boldsymbol{\Phi}_e)^{-1}.$$

$\boldsymbol{\Lambda}_{rel}$ is the relative inertia between the manipulator and the environment—the tensor that relates contact force to relative acceleration. Note that if $\boldsymbol{\Phi}_e = \mathbf{0}$ then $\boldsymbol{\Lambda}_{rel} = \boldsymbol{\Lambda}_0$. Substituting Eqs. 24 and 25 back into Eqs. 22 and 23 gives (the factor $\boldsymbol{\Lambda}_{rel}\,\boldsymbol{\Lambda}_0^{-1}$ disappears if $\boldsymbol{\Phi}_e = \mathbf{0}$)

$$\dot{\boldsymbol{\vartheta}}' = \boldsymbol{\Lambda}_{rel}^{-1}\,\bar{\boldsymbol{\Omega}}_f(\boldsymbol{\Lambda}_{rel})\left(\boldsymbol{\Lambda}_{rel}\,\boldsymbol{\Lambda}_0^{-1}\,\mathbf{f}'\right), \tag{26}$$

$$\mathbf{f}_c = \boldsymbol{\Omega}_f(\boldsymbol{\Lambda}_{rel})\left(\boldsymbol{\Lambda}_{rel}\,\boldsymbol{\Lambda}_0^{-1}\,\mathbf{f}'\right). \tag{27}$$

The applied force has been split into two components by means of the projections $\boldsymbol{\Omega}_f(\boldsymbol{\Lambda}_{rel})$ and $\bar{\boldsymbol{\Omega}}_f(\boldsymbol{\Lambda}_{rel})$, with one component responsible for the manipulator's relative acceleration and the other responsible for the contact force. Although there are an infinite number of force decompositions that are compatible with the kinematics of a contact constraint (given by Eqs. 12–15), there is only one that models the dynamic behavior correctly.

Now let us consider the effect of controlling the manipulator via the following dynamic control structure

$$\mathbf{f}' = \boldsymbol{\Lambda}_0\,\dot{\boldsymbol{\vartheta}}'_{comm} + \boldsymbol{\Lambda}_0\,\boldsymbol{\Lambda}_{rel}^{-1}\,\mathbf{f}_{ccomm}, \tag{28}$$

with $\dot{\boldsymbol{\vartheta}}'_{comm}$ the commanded relative acceleration and $\mathbf{f}_{ccomm}$ the commanded contact forces. This results in the equations of motion

$$\dot{\boldsymbol{\vartheta}}' = \boldsymbol{\Omega}_m(\boldsymbol{\Lambda}_{rel}^{-1})\,\dot{\boldsymbol{\vartheta}}'_{comm} + \boldsymbol{\Lambda}_{rel}^{-1}\,\bar{\boldsymbol{\Omega}}_f(\boldsymbol{\Lambda}_{rel})\,\mathbf{f}_{ccomm}, \tag{29}$$

$$\mathbf{f}_c = \boldsymbol{\Omega}_f(\boldsymbol{\Lambda}_{rel})\,\mathbf{f}_{ccomm} + \boldsymbol{\Lambda}_{rel}\,\bar{\boldsymbol{\Omega}}_m(\boldsymbol{\Lambda}_{rel}^{-1})\,\dot{\boldsymbol{\vartheta}}'_{comm}. \tag{30}$$

If the command inputs are filtered by any pair of motion and force projection matrices, so that $\dot{\boldsymbol{\vartheta}}'_{comm} = \boldsymbol{\Omega}_m(\mathbf{B})\,\dot{\boldsymbol{\vartheta}}'_u$ and $\mathbf{f}_{ccomm} = \boldsymbol{\Omega}_f(\mathbf{A})\,\mathbf{f}_{cu}$, where $\dot{\boldsymbol{\vartheta}}'_u$ and $\mathbf{f}_{cu}$ are the unfiltered command signals, then Eqs. 29 and 30 simplify to

$$\dot{\boldsymbol{\vartheta}}' = \boldsymbol{\Omega}_m(\mathbf{B})\,\dot{\boldsymbol{\vartheta}}'_u, \tag{31}$$

$$\mathbf{f}_c = \boldsymbol{\Omega}_f(\mathbf{A})\,\mathbf{f}_{cu}. \tag{32}$$

(See Eqs. 16–19.) These equations are decoupled in the sense that the relative acceleration depends only on the filtered output of the motion controller, and the contact force depends only on the filtered output of the force controller.

7. Experimental Application of the model

The model can be used in several ways to build force/motion controllers that can deal with contact tasks that go beyond the Raibert-Craig model.

7.1. The experimental testbed

Fig. 3 shows the experimental platform: a dual-arm robotic workcell, consisting of two SCARA-type manipulators and an overhead vision system which tracks the positions of the arms and the objects that they are in contact with. In this experiment, both arms cooperatively grasp a metal rod (approximately 60 cm long). Hinges in the grippers allow the bar to rotate with respect to the end effectors. Each individual arm has four actuated degrees of freedom; both arms together can move the rod in five degrees of freedom. The two end-points of the rod are in contact with the environment, following the configuration of Fig. 1.

A joint-level controller uses joint torque sensors to compensate for (exaggerated) joint-flexibility and the fact that the actuators are not ideal torque sources [14]. The dynamics of the two arms and the manipulated object are combined in the operational space and are of the form of Eq. 20, where $\boldsymbol{\Lambda}_0 = \boldsymbol{\Lambda}_{0l} + \boldsymbol{\Lambda}_{0r} + \boldsymbol{\Lambda}_{0o}$ is the total inertia of the two arms and the manipulated object, $\mathbf{f}$ is the total torque from both arms, and $\mathbf{f}_c = \mathbf{f}_{c1} + \mathbf{f}_{c2}$ is the total effect of the two contacts. Using the transformations of Eqs. 1 to 7, all vectors and matrices are expressed in an operational frame which is (arbitrarily) located in the middle of the rod.

7.2. Decoupled Architecture for Force/Motion Control

Figure 4 shows the global architecture of the force/motion controller. In this implementation, the contact model is represented by a 6×2 matrix $\mathbf{N}$. It is continuously updated as the arms and/or objects move.

7.3. Projection of the measured forces

The 6-dof force-sensors used in this experiment sit between the arm end-points and grippers holding the manipulated object described by the matrix $\boldsymbol{\Lambda}_{0o}$. The measured forces are filtered through the projection matrix $\boldsymbol{\Omega}_f(\boldsymbol{\Lambda}_{0o})$ which depends on the inertia $\boldsymbol{\Lambda}_{0o}$ of the manipulated object. This is necessary to remove the forces that are caused by accelerations of the manipulated object in the tangential space $\mathbf{T}$.

Figure 3. The dual-arm robotic workcell and the two-contact task

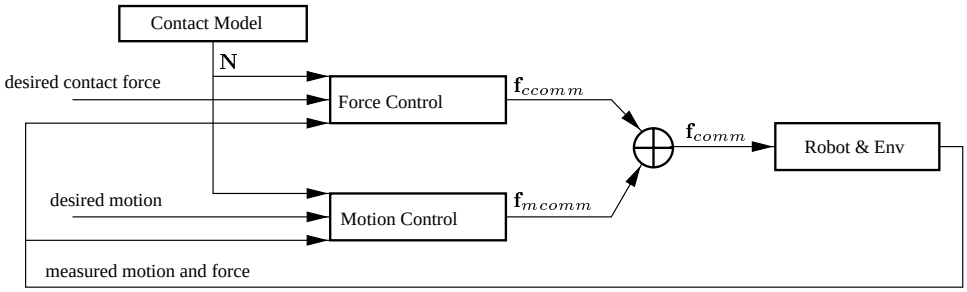

Figure 4. Decoupled Architecture for Force/Motion Control

The experiment of Fig. 5 shows how the reciprocity condition holds when the contact constraints are respected. The top part of the plot is the total instantaneous power $\boldsymbol{\vartheta}^T \mathbf{f}'_{meas}$, which includes the power resulting from object motion. The bottom plot is the power $\boldsymbol{\vartheta}^T (\boldsymbol{\Omega}_f(\boldsymbol{\Lambda}_{0o})\, \mathbf{f}'_{meas})$ delivered by the forces projected in the contact space. In theory, $\boldsymbol{\vartheta}^T \boldsymbol{\Omega}_f(\mathbf{A})$ should be exactly zero for any admissible $\mathbf{A}$; but small kinematic modeling errors produce a slight non-zero value, and this accounts for the non-zero power in the bottom plot.

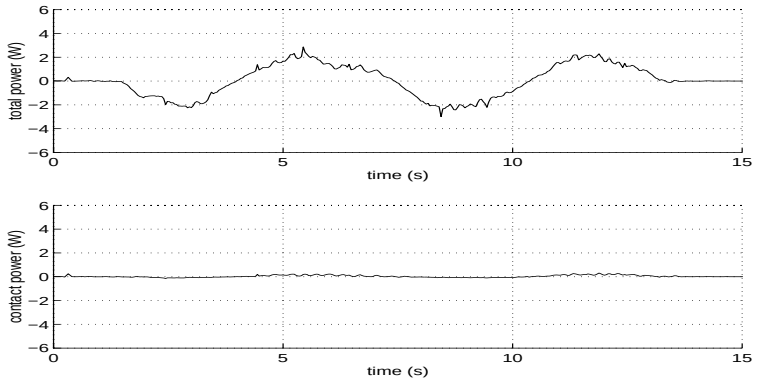

Figure 5. Power with and without projection while contacts are maintained

Figure 6 shows how the reciprocity condition is violated when the constraints are not respected. Every peak corresponds to a collision between the rod and the environment.

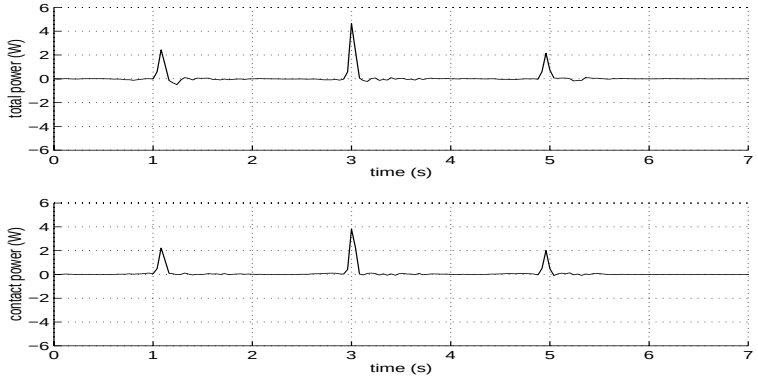

Figure 6. Power with and without projection when contacts are *not* maintained

7.4. Force Control

Fig. 7 shows the basic force control structure. The measured force is first passed through $\mathbf{\Omega}_f(\mathbf{\Lambda}_{0o})$, and the result is projected onto the two-dimensional space of contact normal magnitudes by an arbitrary generalized inverse of $\mathbf{N}$. The contact force controller compares the measured contact forces, $\boldsymbol{\alpha}_{meas}$, with the vector of desired contact force magnitudes, $\boldsymbol{\alpha}_d$, and computes a command vector that is designed to reduce the difference between the two. Finally, the command vector is combined with the desired force vector (used as a feed-forward term), and the result is transformed back to operational space by multiplying by $\mathbf{N}$. From Eq. 29, it is clear that this controller will not disturb the control of motions.

Figure 8 shows the desired and measured contact forces $\mathbf{f}_{c1}$ and $\mathbf{f}_{c2}$. These

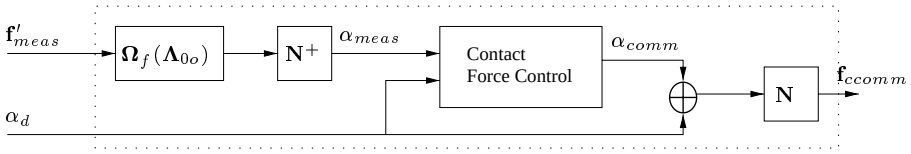

Figure 7. Force Control in the **N** space

forces are controlled in the two-dimensional space N (described by matrix **N**), which can simply not be described by the Raibert-Craig model.

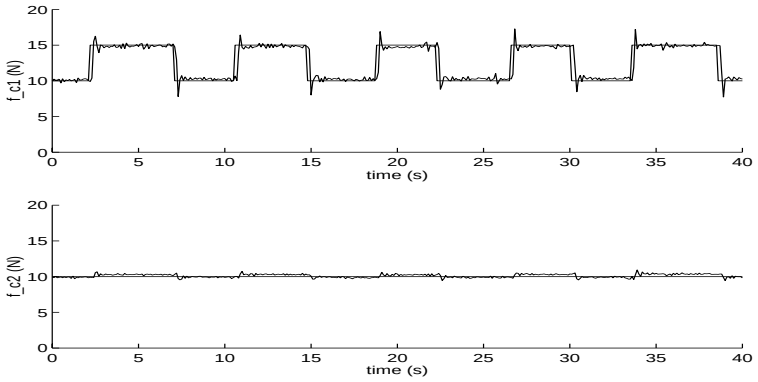

Figure 8. Multi Contact Force Control

8. Conclusion

This paper extends the Raibert-Craig model to a more general framework in which any contact state between the manipulated object and the environment can be described (to first order). This kinematic model can be combined with the dynamics of the arm and the manipulated objects. This approach makes it possible to model and control force/motion tasks that include multiple points of contact which cannot be tackled with the Raibert-Craig model. The experimental results show how the reciprocity condition holds for the projected values of the measured contact forces while the state of contact is maintained and how the results can be used to control forces in multiple points of contact between the robot and the environment.

References

[1] An, C. H., and Hollerbach, J. M., Kinematic Stability Issues in Force Control of Manipulators, IEEE Int. Conf. Robotics and Automation, pp. 897–903, Raleigh, NC, 1987.

[2] Bruyninckx, H., Demey, S., Dutré, S., De Schutter, J., Kinematic Models for

Model-Based Compliant Motion in the Presence of Uncertainty, *Int. Jnl. Robotics Research*, Vol. 14, No. 5, pp. 465–482, 1995.

[3] De Luca, A., and Manes, C., Modelling of Robots in Contact with a Dynamic Environment, *IEEE Trans. Robotics and Automation*, Vol. 10, No. 4, pp. 542–548, 1994.

[4] De Schutter, J., and Van Brussel, H., Compliant Robot Motion I. A Formalism for Specifying Compliant Motion Tasks, *Int. Jnl. Robotics Research*, Vol. 7, No. 4, pp. 3–17, 1988.

[5] Duffy, J., The Fallacy of Modern Hybrid Control Theory that is Based on "Orthogonal Complements" of Twist and Wrench Spaces, *Jnl. Robotic Systems*, Vol. 7, No. 2, pp. 139–144, 1990.

[6] Faessler, H., Manipulators Constrained by Stiff Contact—Dynamics, Control and Experiments, *Int. Jnl. Robotics Research*, Vol. 9, No. 4, pp. 40–58, 1990.

[7] Featherstone, R., *Robot Dynamics Algorithms*, Kluwer Academic Publishers, Boston/Dordrecht/Lancaster, 1987.

[8] Fisher, W. D., and Mujtaba, M. S., Hybrid Position/Force Control: A Correct Formulation, *Int. Jnl. Robotics Research*, Vol. 11, No. 4, pp. 299–311, 1992.

[9] Jankowski, K. P., and ElMaraghy, H. A., Dynamic Decoupling for Hybrid Control of Rigid-/Flexible-Joint Robots Interacting with the Environment, *IEEE Trans. Robotics & Automation*, Vol. 8, No. 5, pp. 519–534, Oct. 1992.

[10] Khatib, O., A Unified Approach for Motion and Force Control of Robot Manipulators: The Operational Space Formulation, *IEEE Jnl. Robotics & Automation*, Vol. 3, No. 1, pp. 43–53, 1987.

[11] Khatib, O., Inertial Properties in Robotic Manipulation: An Object-Level Framework, *Int. Jnl. Robotics Research*, Vol. 14, No. 1, pp. 19–36, 1995.

[12] Lipkin, H., and Duffy, J., Hybrid Twist and Wrench Control for a Robotic Manipulator, *ASME Jnl. Mechanisms, Transmissions & Automation in Design*, vol. 110, No. 2, pp. 138–144, June 1988.

[13] Mason, M. T., Compliance and Force Control for Computer Controlled Manipulators, *IEEE Trans. Systems, Man & Cybernetics*, Vol. SMC-11, No. 6, pp. 418–432, June 1981.

[14] Pfeffer, L. E., and Cannon, R. H., Experiments with a Dual-Armed, Cooperative, Felxible-Drivetrain Robot System, IEEE Int. Conf. Robotics and Automation, pp. 601–608, Atlanta, GA, 1993.

[15] Raibert, M. H., and Craig, J. J., Hybrid Position/Force Control of Manipulators, *ASME Jnl. Dynamic Systems, Measurement & Control*, Vol. 103, No. 2, pp. 126–133, June 1981.

[16] West, H., and Asada, H., A Method for the Design of Hybrid Position/Force Controllers for Manipulators Constrained by Contact with the Environment, IEEE Int. Conf. Robotics and Automation, pp. 251–259, St. Louis, MO, 1985.

[17] Yoshikawa, T., Sugie, T., and Tanaka, M., Dynamic Hybrid Position Force Control of Robot Manipulators — Controller Design and Experiment, *IEEE Jnl. Robotics & Automation*, Vol. 4, No. 6, pp. 699–705, 1988.

[18] Zhang, H., Kinematic Stability of Robot Manipulators under Force Control, IEEE Int. Conf. Robotics and Automation, pp. 80–85, Scottsdale, AZ, 1989.